2020

Diclofenac Determination Using CeO2 Nanoparticle Modified Screen-printed Electrodes:a Study of Background Correction

Rafaela C. de Carvalho
Tecnnological University Dublin

Tony Betts
Technological University Dublin, anthony.betts@tudublin.ie

John Cassidy
Technological University Dublin, john.cassidy@tudublin.ie

Recommended Citation

de Carvalho, R. C., Betts, A & Cassidy, J.F. (2020). Diclofenac determination using CeO2 nanoparticle modified screen-printed electrodes:astudy of background correction. *Microchemical Journal*, vol.158, 105258. doi:10.1016/j.microc.2020.105258

Microchemical Journal 158 (2020) 105258

Contents lists available at ScienceDirect

Microchemical Journal

journal homepage: www.elsevier.com/locate/microc

Diclofenac determination using CeO_2 nanoparticle modified screen-printed electrodes – A study of background correction

Rafaela C. de Carvalho[a,b,*,1], Anthony J. Betts[a,1], John F. Cassidy[a,b,1]

[a] Applied Electrochemistry Group, FOCAS Research Institute, Technological University Dublin, City Campus, Kevin Street, Dublin DO8 NF82, Ireland
[b] School of Chemical and Pharmaceutical Sciences, Technological University Dublin, City Campus, Kevin Street, Dublin D08 NF82 Ireland

ARTICLE INFO

Keywords:
CeO_2
Screen Printed Carbon Electrodes
Background correction
Square Wave Voltammetry

ABSTRACT

The detection of low levels of drugs including Non-Steroidal Anti-Inflammatory Drugs (NSAIDs) in natural waters and wastewaters is becoming increasingly important. Electrochemical methods offer an attractive means of detection, as they overcome many disadvantages associated with the currently available analytical methods. Cerium dioxide nanoparticles were synthesised and then incorporated onto the working electrodes of commercial graphite-based Screen Printed Carbon Electrodes (SPCE) then used to determine diclofenac levels. Following initial Cyclic Voltammetry studies, Square Wave Voltammetry (SWV) investigations were conducted over a range of conditions to optimise the peak potential separation and sensitivity of the method. The use of background correction as signal processing is highlighted since it constitutes a mandatory pre-treatment of data before the analysis of results. SWV study was carried out on diclofenac over a concentration range from 0.4 μM up to 26 μM which indicated that the response was linear with a limit of detection of 0.4 μM and a sensitivity of 0.058 μA/μM. The SWV method provides a rapid means of diclofenac detection where cerium dioxide nanoparticles combined with electrode vacuum heat treatment and use of background correction all play an important role.

1. Introduction

In the last decade, the investigation and use of electrochemical techniques in the analysis of pharmaceuticals drugs and other compounds have shown promising results. Such compounds and their degradation products may accumulate in an ecosystem causing harmful environmental damage. There is a wide range of analytical techniques available for quantification of pharmaceutical compounds, notably spectrophotometric and chromatographic techniques such as UV–Visible, Raman spectroscopy, Mass spectrometry, High-Performance Liquid Chromatography, Liquid Chromatography-Mass Spectrometry and Gas Chromatography among others [1,2]. When compared with other analytical techniques, electrochemical methods provide simple, rapid, selective detection using relatively low-cost instrumentation.

The efficacy of the electrochemical methods is largely determined by the electron transfer capability of the working electrode surface. Therefore, to improve the electrochemical performance of this electrode, a typical strategy is to design composites combining electrocatalytically active materials with conductive additives to modify the working electrode surface. Numerous materials have been developed with carbon-based materials showing particular promise. These include boron-doped carbon diamond electrodes (BDDE) [4], glassy carbon electrodes [5], carbon paste electrodes [3], graphene electrodes [6], modified glassy carbon electrodes and screen-printed carbon/graphite electrodes (SPCE) [7,8]. Currently, such SPCE find applications in diverse areas of electrochemistry; however, it has been used most often in the bioelectrochemical field for sensing applications [8,9].

The use of catalyst materials to improve the stability and conductivity of the WE has become an area of increasing interest for electroanalysis [5]. Diclofenac 2-[(2,6-dichlorophenyl)amino] benzene acetic acid sodium salt or DCF is well known as a Non-Steroidal Anti-Inflammatory Drug (commonly abbreviated as an NSAIDs) and is often used as an analgesic [10,11]. Due to its widespread use, diclofenac residues can be found in seawater, rivers and lakes [12–14]. Diclofenac and its residues have been identified as compounds of concern in aquatic systems particularly when accumulated and combined with by-products of DCF and other pharmaceuticals drugs [15]. Thus, the development of an electrochemical method for the detection of diclofenac and its degradation products along with many other pharmaceutical substances in-situ is extremely important for environmental monitoring. Electrochemical techniques using modified electrodes have

* Corresponding author.
E-mail address: rafa_cdc@homail.com (R.C. de Carvalho).
[1] Rafaela C. de Carvalho - ORCID: 0000-0003-0849-110X, Anthony J. Betts - ORCID: 0000-0003-1544-5152, John F. Cassidy - ORCID: 0000-0002-7081-8268.

https://doi.org/10.1016/j.microc.2020.105258
Received 15 May 2020; Received in revised form 5 July 2020; Accepted 5 July 2020
Available online 10 July 2020

been investigated for the estimation of levels of easily oxidised organic molecules such as diclofenac (DCF), acetaminophen (paracetamol ACOP), aspirin (acetylsalicylic acid, ASA), cocaine (COC), codeine (COD) and caffeine (CAF) when presented individually, as well as their simultaneous determination in certain pharmaceutical formulations [3,10,16,17]. For example, a research group from Brazil developed a working electrode using BDDE and Square Wave Voltammetry (SWV) for the determination of COC and screening of the most common adulterants (benzocaine, caffeine, lidocaine, phenacetin, paracetamol, and procaine) in seized COC samples [4]. Khairy et al. developed a screen-printed electrode coated with cerium dioxide (CeO_2) nanoparticles (NPs) which were utilised for the simultaneous detection of ACOP, COD and CAF using differential pulse voltammetry (DPV) and enhanced electron transfer rates of the WE wereobserved [18]. Cerium dioxide, both undoped and doped with boron and with indium was also employed in a range of electrochemical sensors reported by Ibrahim and Temerk [19–22]. These were developed to detect a number of organic compounds of biomedical interest, including megestrol acetate, xanthine, hypoxanthine and uric acid in human biological fluids, such as human serum and urine and fish meat samples. Another paper describing the use of Co-doped CeO_2 nanoparticles to detect the biological compounds xanthine, hypoxanthine and uric acid was also described by Lavanya et al. [23].

For analytical purposes, SWV is usually the ideal method for analysis as it suppresses the background (non-faradaic or capacitive) current effectively and also has higher sensitivity compared to other electrochemical techniques [24,25]. This method often leads to increases in analyte peak height and enables much faster scan rates into the Vs^{-1} range to be employed while diminishing the non-faradaic charging contribution [26]. In this work the use of CeO_2 NPs modified SPCEs in conjunction with SWV for the detection of DCF is shown to be beneficial. Towards this goal, a novel and simple precipitation synthesis of CeO_2 NPs was initially developed and then investigated using both Cyclic Voltammetry (CV) and SWV techniques in aqueous conditions pertinent to the analysis of DCF in environmental water samples, but not in pharmaceutical products or biological fluids. The role of background current correction which is especially important at higher potential values is also explored.

2. Experimental

2.1. Chemicals

Sodium diclofenac, monosodium phosphate and disodium phosphate (all of analytical grade) were purchased from Sigma-Aldrich Company and used without further purification. The other chemicals used were acetic acid 99.5%, boric acid 99%, hydrochloric acid 37%, phosphoric acid 98%, sodium hydroxide pellets and potassium ferrocyanide 99%. All were obtained from Fisher Scientific. The CeO_2 nanoparticles (NP) were synthesised, with a size range of 27–52 nm and a uniform morphology with well-defined spherical shape (see supplementary information, , Fig SI-1). Solutions were prepared using ultrapure water (18.2 MΩ cm). Britton-Robinson buffer solutions (BRB) (pH ranging between 2.0 and 12.0) were utilised as the electrolyte. The pH was adjusted using either 2 M NaOH or 0.2 M HCl solution.

2.2. Instrumentation

The voltammetric measurements (both CV and SWV) were performed on an Eco Chemie B.V, Electrochemical Work Station, model Autolab PGSTAT 12 (The Netherlands) using GPES software (version 4.9). All measurements were conducted using a three-electrode one compartment configuration, in which the working electrode was a graphite-based screen-printed electrode with a geometric area of 4 mm diameter, and 15 ± 4 μm thickness. These screen-printed electrochemical sensors (SPCE) were purchased from Methohm-DropSens, model DRP-110 with dimensions: 3.4 × 1.0 × 0.05 cm (Length × Width × Height). The counter electrode consisted of a graphite film, and a silver pseudo-reference electrode was also part of the three-electrode system. However, to avoid any interference due to the instability of the reference electrode (Ag-serves as a pseudo-reference electrode in this SPCE), an external reference electrode was utilised instead (Hg/Hg_2Cl_2, KCl (sat'd) – saturated calomel electrode (SCE) (from Radiometer model REF421). A Labquest2 digital pH meter was utilised together with a calibrated pH electrode to measure the pH of solutions. A Gallenkamp (from Fistreem International Ltd) vacuum oven was used at 7.6 torr for further treatment of the sensors.

2.3. Preparation of the modified electrode (SPCE-CeO_2)

In order to overcome some inherent variability in responses between different SPCEs, all SPCEs were subjected to an electrochemical pre-treatment (EP). This was done in an attempt to remove impurities and thus improve their electroactivity, and also to alter the SPCE WE surface wettability. A potential of +1.4 V (vs. SCE) was initially applied for 300 s in 0.05 M phosphate buffer solution (pH 7.2) to each SPCE WE, after which it was rinsed with deionised water. Such a pre-treatment has been reported previously [27–29]. For example, Moreno et al. reported that the EP can also prove beneficial through the introduction of new electrochemically active sites by removing impurities on the SPCE active working electrode surface [29].

A suspension of the synthesised CeO_2 NP annealed at 900 °C (see supplementary information, , Fig SI-2) was prepared by adding 0.5 mg of NPs in 1 mL of ultrapure water. The temperature of 900 °C was chosen based on the data provided in the supplementary information. Following the SPCE pre-treatment, 5 μL of this suspension was then drop cast directly on the WE surface of the SPCE by a micropipette and the sensor was then subjected to a heat treatment in a vacuum oven operating at 7.6 torr for 1 h at 100 °C, thus completing the preparation of the modified SPCE-CeO_2. A summary of the procedure is shown in the flowchart in Fig. 1.

This vacuum heat treatment (VHT) was necessary to allow the NPs to strongly adhere to the WE surface causing the binder present in the SPE to melt and flow on the WE, thus avoiding dislodgement during the subsequent electrochemical analysis. Scanning electron microscopic images of the sensor surfaces were used to compare the morphological features of the WE surface of the screen-printed electrode, before and after adding the CeO_2 NP. The SEM image of a bare SPCE, Fig. 2(a) indicated a porous, highly faceted structure. In contrast, the relatively smooth surface observed for the drop cast WE surface presented in

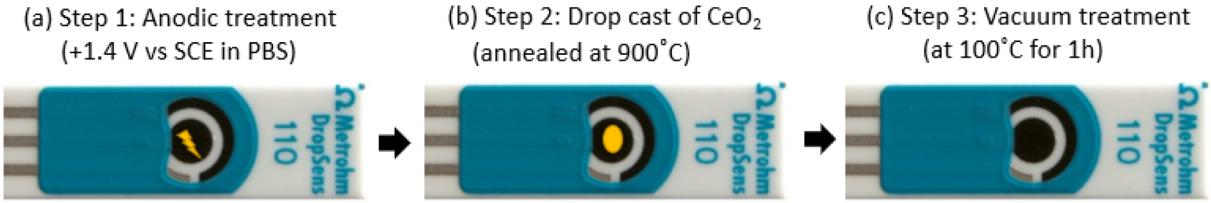

Fig. 1. (a) Illustration of the EP performed at SPCE. A potential of +1.4 V (vs. SCE) was applied for 300 s in 0.05 M phosphate buffer solution (pH 7.2) to the WE (b) CeO_2 annealed at 900 °C was prepared by adding 0.5 mg of NPs in 1 mL of ultrapure water. 5 μL of this suspension was then drop cast directly on the WE surface (c) thermal treatment in a vacuum (7.6 torr) oven for 1 h at 100 °C, thus completing the preparation of the modified SPCE-CeO_2.

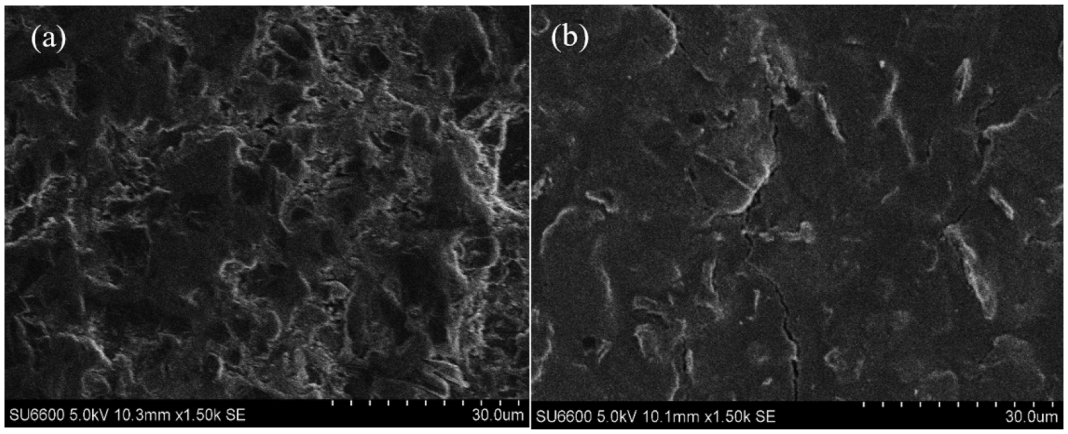

Fig. 2. (a) Scanning electron micrographs of untreated carbon-based working electrodes (b) and after drop-casting with CeO_2 NPs annealed at 900 °C and VHT at 100 °C for 1 h.

Fig. 2(b) was possibly due to the CeO_2 NP filling the graphite gaps and thus causing the smoother surface. Similar results have also been reported by Kadara et al. whereby a comparison between different electrochemical platforms was carried out [27]. All experiments were conducted at room temperature (22–25 °C) using a fresh electrode (SPCE) for each analysis. Moreover, all solutions were stirred for 60 s with an equilibration time of 30 s between each consecutive analysis.

2.4. Acquisition and presentation of voltammetric data

All results obtained by SWV are presented after a baseline-correction using the "moving average" algorithm (peak width = 0.03 V) included in the Autolab GPES software (version 4.9.007). This version can be found on the metrohm website (https://www.ecochemie.nl/) and is very effective when peaks appear as shoulders on steep flanks. After baseline correction, individual peaks can often be seen far more clearly. The curve fitting approaches are usually created using the simulation of a complex signal and the sum of single peak models, utilising least-squares minimization as reported by Jakubowska et al. [30].

This mathematical treatment improves the imaging and identification of the peaks above the baseline without the introduction of artefacts, although the peak current is in some cases decreased slightly (< 10%) compared to that of the untreated curve [30]. In the quantitative voltammetric analysis, the peak height (the maximum current with respect to the baseline) is the most widely used parameter to determine concentrations. This parameter will, therefore, be utilised for further calculation [24].

3. Results and discussion

3.1. Cyclic voltammetry characterisation of the modified electrode

In order to determine and compare the electrochemically active surface area (EASA) of the SPCE-CeO_2, and the SPCE, a CV was conducted at 0.05 Vs^{-1} in a solution of 5 mM $K_4Fe(CN)_6$ in 0.1 M KCl. The electrochemical reaction of $K_4Fe(CN)_6$, is described according to the following equation for a quasi-reversible electron transfer process; the modified-quasi-reversible Randles– Ševčik (RS) equation [31]:

$$I_p = (2.99 \times 10^5)n^{3/2}\alpha^{1/2}AD^{1/2}C\,\nu^{1/2} \quad (1)$$

where I_p, n, α, A, D, C,ν are peak current in amps, n is the number of electrons transferred (n = 1 for $[Fe(CN)_6]^{3-}/[Fe(CN)_6]^{4-}$), α is the transfer coefficient (usually taken to be close to 0.5), electrochemically active surface area (cm^2), diffusion coefficient ($cm^2\ s^{-1}$), concentration of ferrocyanide (mol/cm^3) and scan rate ($V\ s^{-1}$), respectively. The diffusion coefficient of potassium ferrocyanide is $6.3 \times 10^{-6}\ cm^2\ s^{-1}$ at 25 °C [31]. A typical CV is shown in Fig. 3, obtained at a scan rate of 0.05 Vs^{-1} and the resultant anodic peak current was used to calculate the EASA using the Randles–Ševčik (Eq. (1)). An alternative approach using the potential step (chronoamperometric) technique in conjunction with the Cottrell equation is often used to assess the EASA [32]. For an inner sphere reactant however such as potassium ferrocyanide or ascorbic acid, they showed that both approaches were comparable. Other recent investigations utilising the CV/Randles-Ševčik approach described herein have also been reported [19–22,32–35].

The original carbon surface of VHT SPCE (bare) is characterised by a large number of edges of graphite particles and a rather porous, rough surface as can be seen in Fig. 2. However, the modified SPCE-CeO_2 is far smoother in appearance and perhaps the nanoceria along with the heat treatment, made the WE surface more conductive with enhanced electron transfer rates. Such a statement can be confirmed with a better current response recorded in the voltammogram for the SPCE-CeO_2 electrodes.

The effective area of a bare SPCE and SPCE-CeO_2 was evaluated in order to compare the EASA for both electrodes. It has been reported that the WE active areas of SPCE from these DropSens SPCE are exposed edge plane-like sites/defects formed during its fabrication, and such changes can affect the roughness of the electrode surface [31,36]. Table 1 indicates the electrochemically active surface area of SPCE-CeO_2 and SPCE. It can be observed that the geometrical area of the

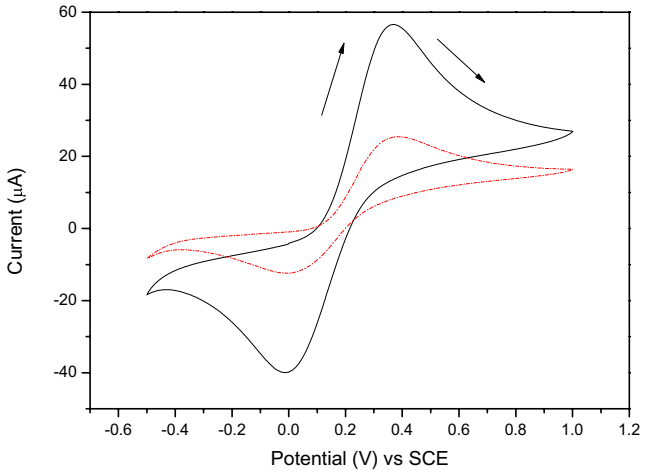

Fig. 3. Typical cyclic voltammogram recorded in 5 mM potassium ferrocyanide in 0.1 M KCl supporting electrolyte at a VHT SPCE (bare) (dashed line) and VHT SPCE-CeO_2 (solid line) obtained at a scan rate of 0.05 Vs^{-1}. The CE was carbon ink and an external SCE served as a RE.

Table 1
A comparison of the electrochemical and geometrical surface area of the SPCE-CeO_2 and SPCE.

	Electrochemical Area A (cm^2)	Geometrical surface area WE $(cm)^2$
SPCE	0.0361	0.1256
SPCE-CeO_2	0.0833	0.1256

SPCE is 3.5 times greater than the EASA. This strongly suggests that SPCE contain only a small fraction of their surface which is electrochemically active, which is most likely to be edge plane graphite flakes protruding above an inert (non-conductive) polymeric binder matrix.

For reversible and quasi-reversible redox reactions such as the potassium ferrocyanide/ferricyanide (hexacyanoferrate II/III) couple, the heterogeneous rate constant k^o can be estimated using Nicholson's method [37]. For a single electron transfer, this is described by Eq. (2) below. In this method, the dimensionless rate parameter Ψ is expressed as:

$$\Psi = \frac{k^0}{[\pi\, Dv\,(F/RT)]^{1/2}} \cdot \gamma^{\alpha/2} \tag{2}$$

where D is the diffusion coefficient of the ferrocyanide species, α is the transfer coefficient, ν is the scan rate and F, R, T has the normal meanings. In addition, γ is given by:

$$\gamma = \frac{D}{D'} \tag{3}$$

where D' is the ferricyanide ion's diffusion coefficient (7.6×10^{-6} cm^2 s^{-1}) [31,38]. For this redox couple then γ is equal to 0.83.

Using the cyclic voltammogram of 5 mM $K_4[Fe(CN)_6]$ in 0.1 M KCl at the SPCE and SPCE-CeO_2 NP electrode obtained at a scan rate of 0.05 V s^{-1} displayed in Fig. 3, the measured value of ΔE_p was 360 mV for both VHT electrodes.

Swaddle developed an empirical equation for Ψ estimation from ΔE_p [39]

$$\ln \Psi = 3.69 - 1.16 \ln(\Delta E_p - 59) \tag{4}$$

For a ΔE_p of 360 mV this generates a value of Ψ of 0.0534. Hence a value of k^0 of 3.4×10^{-4} cm s^{-1} is determined for the potassium ferrocyanide/ferricyanide couple at a sweep rate ν of 0.05 V s^{-1}.

This value of k^0 is comparable to those reported by Morrin et al. who quoted values of less than 10^{-4} cm s^{-1} for two commercial SPCEs displaying very large ΔE_p values (over 400 mV) [38]. They attributed their large SPCE ΔE_p values to poor charge transfer characteristics and hence measured low k^0 values. In the present work, the peak separation value (ΔE_p of 360 mV) is also very large, beyond the range of values of (61–212 mV) tabulated by Nicholson, including those used for quasi-equilibrium conditions.

Curiously the consistent value of k^0 found in our work for both SPCE and SPCE CeO_2 NP seems to suggest that the CeO_2 NP does not affect the rate of electron transfer at the WE. This cannot be the case however, as the higher currents obtained in the SPCE-CeO_2 NP electrode displayed in Fig. 3 attest. There are a number of possible reasons for the existence of large ΔE_p values in SPCEs leading to low k^0 values ($< 10^{-3}$ cm s^{-1}). Aside from the poor internal charge transfer characteristics of the VHT SPCE, the existence of an ohmic drop (uncompensated resistance) may be the reason, a fact recognised by Nicholson where an additional correcting factor is suggested in an amended version of Eq. (1) [37]. Stevens et al. investigated this in a range of conditions including those without added supporting electrolyte recommending use of high concentrations (50 mM) of potassium ferrocyanide/ferricyanide [31].

Another explanation for such high peak separations is the conduction of the CV sweeps in aerated (oxygenated) conditions. For example significantly smaller ΔE_p values of less than 100 mV yielding k^0 values of 5.7×10^{-3} cm s^{-1} and 5.76×10^{-3} cm s^{-1} in a potassium ferrocyanide/ferricyanide redox couple on similar commercial SPCEs to those studied in this work were reported using deaerated electrolytes [40,41]. In contrast high ΔE_p were obtained in this work and others conducted in aerated conditions [38]. Under such oxidising conditions it may be that formation of Prussian Blue $Fe_4[Fe(CN)_6]_3$, (iron(III) hexacyanoferrate(II)) occurs, passivating the electrode surface [42,43].

Finally, it is worth noting that both the SPCE and SPCE-CeO_2/NP electrodes were subjected to a vacuum heat treatment before each CV sweep. Melting of the binder during the VHT in the electrodes leading to flow of the polymer matrix may have caused different surface

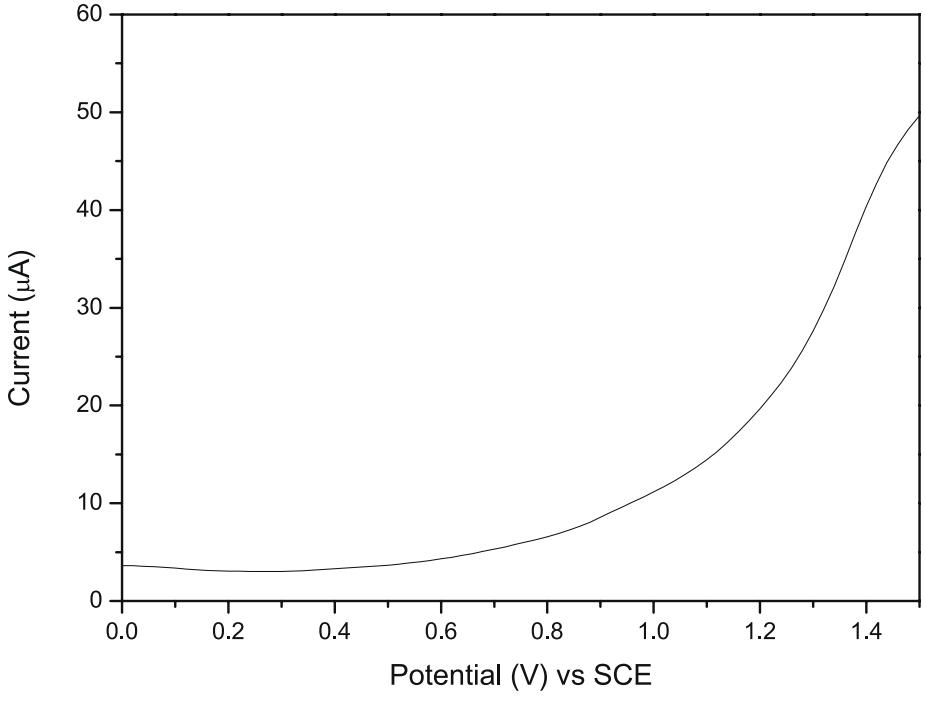

Fig. 4. Square Wave Voltammogram showing the background current on an SPCE-CeO_2 WE in BRB (pH = 7) as a function of potential. SWV conditions: f = 10 Hz, E_{step} = 10 mV and E_{pulse} = 25 mV. Scan conducted from 0 to 1.5 V at a rate of 0.05 Vs^{-1} (scan rate determined by the E_{step} and the frequency). The CE was carbon ink and an external SCE served as a RE.

adsorption characteristics and re-orientation of the conductive graphite flakes within the electrodes.

An SWV plot of background current of the BRB pH 7 (blank) after the EP treatment of an SPCE-CeO_2 is shown in Fig. 4. The parameters used in the SWV were a frequency of 10 Hz, potential step height of 10 mV and pulse height of 25 mV [26]. In this work, these conditions were optimised to improve the sensitivity and quality of the signal of the compounds to be analysed. The high overpotential for oxygen evolution (above +1.0 V) and possibly the instability of carbon electrodes under oxidising conditions invariably leads to a high background current, notably at higher potential values which could adversely affect the baseline correction at high potentials [44,45]. Such high background currents have also been observed at high potentials for other SPCE [3,18].

3.2. Electrooxidation of diclofenac

The electrochemical behaviour of DCF at the surface of the modified screen-printed electrode was investigated initially utilising the CV technique. CV scans were obtained in 100 μM DCF solution in 0.1 M BRB at pH 7 in the potential range from −0.4 to 0.8 V (vs SCE) at a scan rate of 0.05 V s^{-1} and is shown in Fig. 5. A comparison was made between bare-SPCE (a) and the modified screen-printed electrode (a), with the CVs displayed in Fig. 5. The formation of an anodic peak (I_a) with the highest current at about 0.60 V (vs. SCE), is most probably due to the oxidation of the anionic form of DCF as the pKa is 4.18 and sodium salt was utilised in the CV resulting in the initial formation of a radical nitrogen species [46,47]. As the potential first scan was reversed, a cathodic peak (II_c) was observed at 0.26 V (vs. SCE). Aguilar-Lira et al. proposed that this peak corresponds to the reduction of 2-(2-hydroxyphenyl) acetic acid to 1-hydroxy-2-(hydroxyphenyl) ethanoate [48], although at pH 7 it is likely to be the acetate rather than the acetic acid form that is reduced. During the second and subsequent sweeps, a new anodic peak (II_a) appears at 0.34 V (vs. SCE). This indicates that peaks II_a and II_c are related to the same redox process [48]. Thus in the case of multiple scans peak II_c appears which upon the next forward scan oxidises, producing peak II_a. This process is described in the supplementary information, , scheme SI-1 showing the initial formation of a nitrogen radical DCF species.

The voltammogram in Fig. 5 confirms the existence of a higher peak current for the modified electrode, which is likely due to the incorporation of CeO_2 nanoparticles increasing the electrochemically active surface area of the working electrode and also enhancing the electrocatalytic activity of the CeO_2 sensor for electrooxidation of the DCF molecule. DCF is irreversibly oxidised and thus there is no reverse peak associated with peak I_a. Such behaviour has also been reported elsewhere [6,11–13]. Since the peak (I_a) displays the highest current intensity (6.7 μA) and possesses better definition, it was chosen as an analytical signal for DCF quantification. It is worth noting that Aguilar-Lira et al. [48] selected peak II_a in their analysis which was closely associated with another peak II_c as part of a redox couple. In contrast peak I_a is an irreversible peak which is not associated with a comparable cathodic peak. It is also worth noting that in the presence of the CeO_2 nanoparticles another anodic peak (III_a) is evident at approximately 0.46 V (vs SCE) whilst a peak III_c occurs at about −0.05 V (vs SCE). This peak has not been reported before and is obviously associated with the CeO_2 NPs, as it is not present in the CV of the unmodified (bare) SPCE. Although the reactions responsible for the well-separated peaks are uncertain, one possibility is the formation of a polyaniline-like conducting polymer [49]. According to the reaction scheme proposed by both Cid-Cerón et al. [47] and Aguilar-Lira et al. [48], one of the products following the initial formation of the dehydrogenated nitrogen radical in the initial single electron transfer oxidation step is 2,6-dichloroaniline. Possibly catalysed by the CeO_2 NPs on the modified SPCE, this may then react to form a poly-dichloroaniline species, although further work is required to confirm this. Alternatively, it could be a reaction involving one of the DCF degradation species reported by Brillas et al. in their study of the anodic treatment of DCF solutions [50].

Enhanced reactivity of SPCE-CeO_2 after VHT could also possibly be explained by an increase of oxygen vacancies on the CeO_2 surface. Such behaviour can change the concentration and recombination ratio of

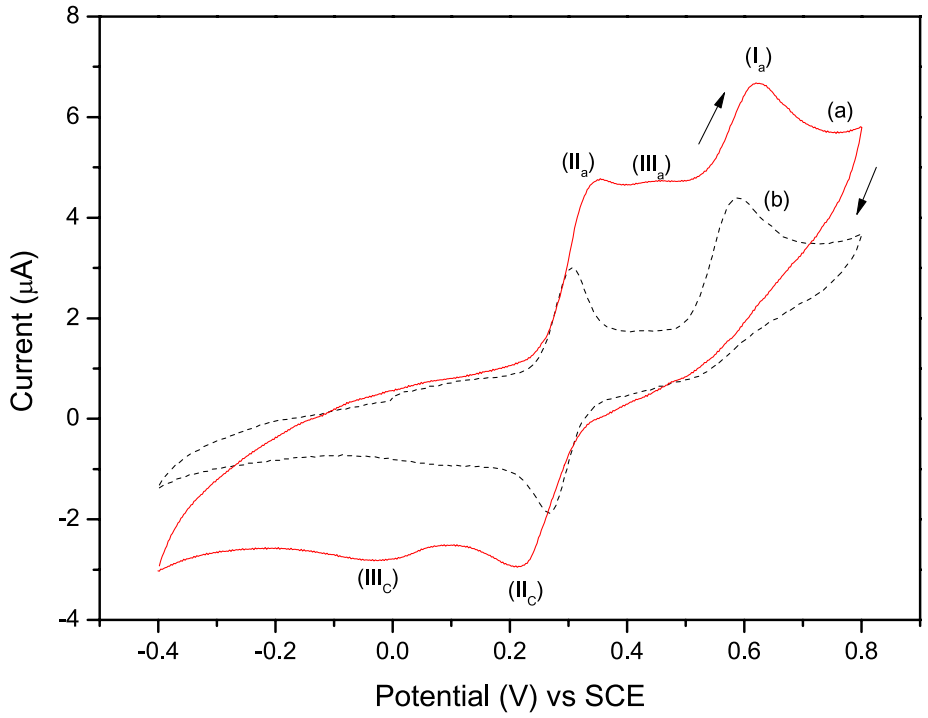

Fig. 5. Cyclic voltammograms (CVs) of 100 μM of DCF solution in BRB (pH 7) at (a) Modified SPCE-CeO_2 (solid line) and (b) Bare-SPCE (dashed line). The potential ranged from −0.4 to 0.8 V (vs SCE) at a scan rate of 0.05 Vs^{-1}. The SPCE-CeO_2 is the WE. The CE was carbon ink and an external SCE served as a RE.

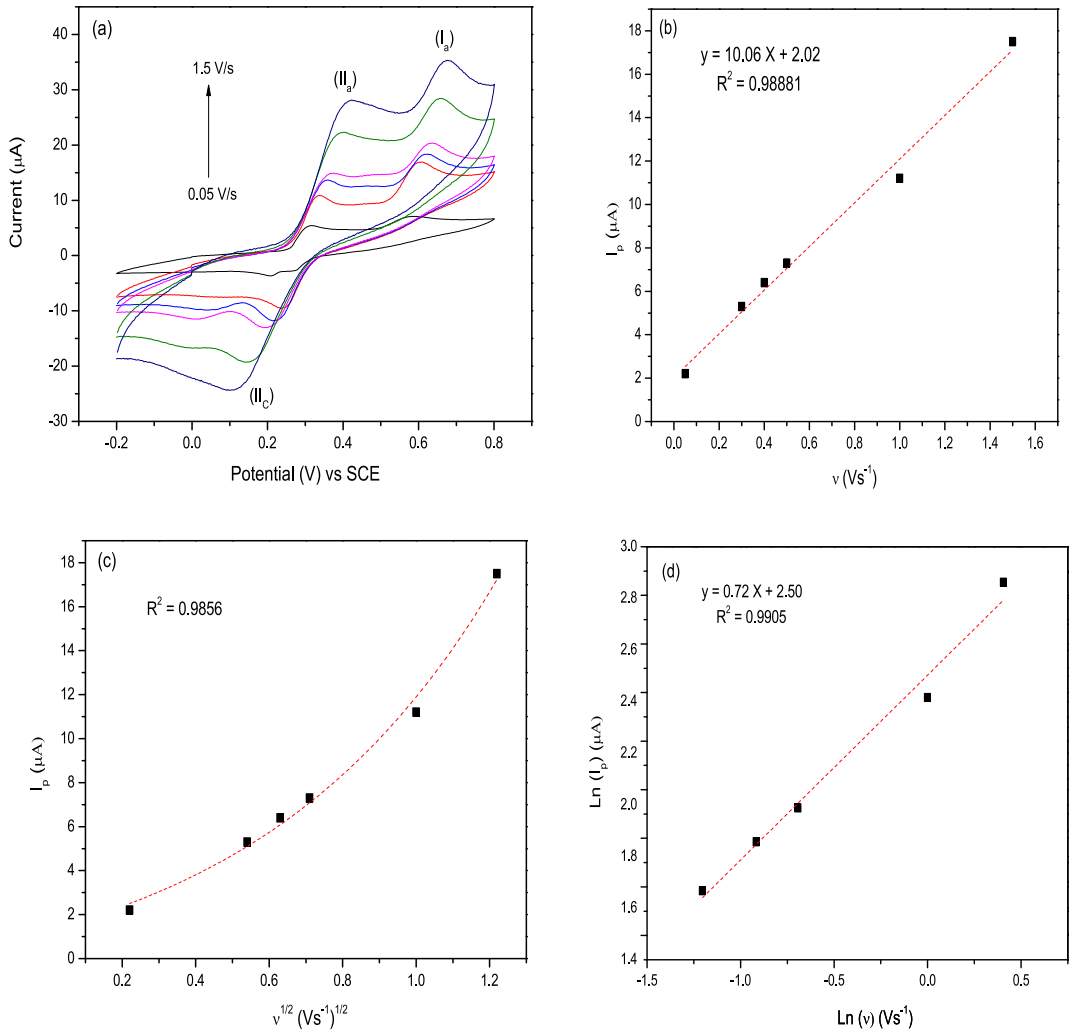

Fig. 6. (a) Cyclic voltammograms of DCF at SPCE-CeO_2 at different scan rates from 0.05 to 1.5 Vs^{-1} in BRB (pH = 7) and [DCF] = 100 μM. The SPCE-CeO_2 is the WE. CE was carbon ink and the external SCE was the RE. (b) Plot of I_p (from peak I_a) vs. ν with background correction for the oxidation of DCF at SPCE-CeO_2. (c) Plot of I_p vs. $\nu^{1/2}$ with background correction for the oxidation of DCF at SPCE-CeO_2. (d) Plot of Ln (I_p) vs. Ln (ν) with background correction for the oxidation of DCF at SPCE-CeO_2.

Ce^{4+} and Ce^{3+} species (see supplementary information, Fig SI-3) and in addition may introduce further levels of point defects due to the highly defective nature of the nanosized CeO_2 [51]. Choudhury et al. reported that annealing (at 100 °C) of CeO_2 NPs under vacuum introduces Ce^{3+} and oxygen vacancies in the CeO_2 lattice sites and on the crystal surfaces as well as on the grain boundaries. [52]. Such properties can enhance the catalytic performance of CeO_2, especially on the nanoscale. Thus the incorporated CeO_2 NPs stabilised the SPCE surface and promoted higher catalytic activity and enhanced sensor response.

3.2.1. Effect of scan rate

In order to better understand the nature of the reaction and the role of the potential sweep rate on the oxidation peak current (I_p of peak I_a) of DCF, CVs were performed at various selected scan rates in the range 0.05–1.5 V s^{-1}. As shown in Fig. 6 (a), the anodic peak current of peak I_a increases with increasing scan rate and a slight shift in the oxidation peak potentials (E_p) occurs towards more positive values.

A linear relationship was observed between the anodic peak current (with background correction) and the scan rate (I_p vs. ν) in Fig. 6 (b). This indicates that the DCF oxidation process on the CeO_2 modified screen-printed electrode is adsorption-controlled [24,25]. A plot of I_p vs. $\nu^{1/2}$ shown in Fig. 6(c) is clearly curved (ie. non-linear). Finally, a plot of ln (I_p) vs ln v (Fig. 6(d)) is also linear, with a slope of 0.72, for sweep rates above 0.05 V/s. A slope of 0.5 in such double logarithm plots is thought to indicate a semi-infinite diffusion process, whilst a finite (thin layer) diffusion process possesses a slope of 1.0 [13]. Thus a slope of 0.72 probably indicates the occurrence of a mixed process [40,53]

This suggests that an adsorbed species is involved and therefore peak I_a is not solely due to a diffusion-controlled reaction involving a solution-based molecule. Costa-Rama et al. reported that there are regions exposed to the bulk solution in which planar diffusion operates and a region in which "thin layer" diffusion effects occur for a carbon-based WE [54]. As indicated in Fig. 6(a), a reverse peak for peak I_a is often absent, apart from some scan rates (0.4 V/s, 0.5 V/s and 1.0 V/s) in which a peak appears at about −0.02 V (vs SCE) to 0.05 V (vs SCE) which is far apart from the peak I_a at about 0.6 V(vs SCE) to 0.7 V (vs SCE). This indicates that the electron transfer reaction associated with peak I_a is essentially irreversible [55].

With the knowledge that the oxidation reaction of DCF probably involves an adsorbed surface species process involving a single electron transfer, resulting in the formation of an adsorbed nitrogen radical, it is possible to estimate the heterogeneous rate constant k^0. Originally proposed for an irreversible reduction of an adsorbed species by Laviron [56], this was later summarised in a review by Honeychurch and Rechnitz [57] who provided three diagnostic criteria for the

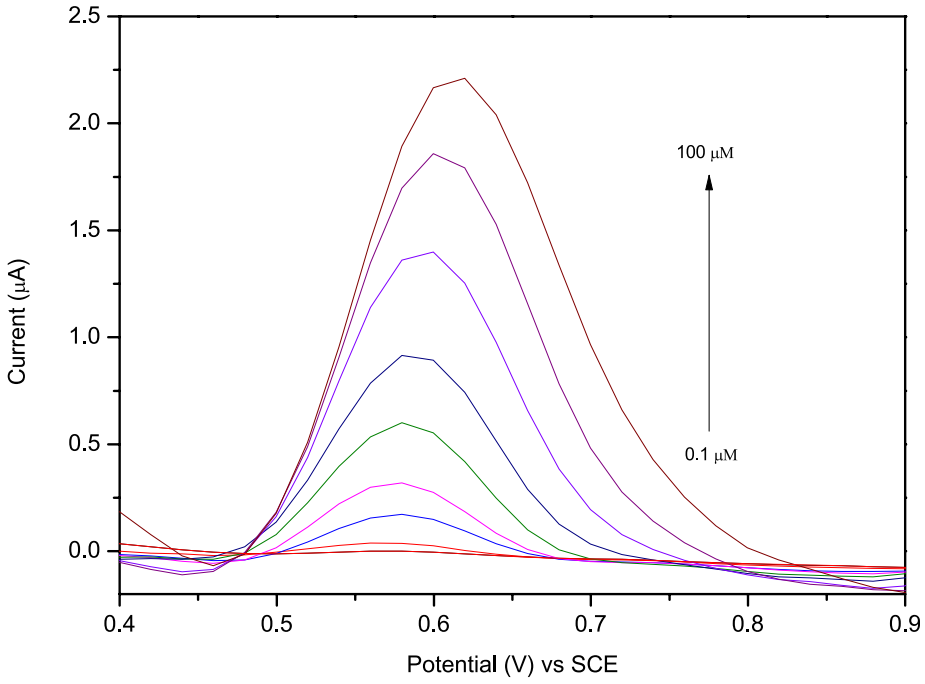

Fig. 7. Square wave voltammograms of DCF at different concentrations in the range 0.1–100 μM. The SPCE-CeO_2 is the WE. A carbon ink CE and an external SCE was the RE. SWV was performed under the optimum parameters. Analysis conditions: f = 40 Hz, E_{step} = 20 mV and E_{pulse} = 25 mV. SWV performed in BRB (pH = 7).

voltammetry of an adsorbed redox species undergoing irreversible adsorption kinetics.

(i) Linear plot of I_p vs v (as displayed in Fig. 6(b))
(ii) Plot of E_p vs ln v should also be linear with a slope of ($RT/\alpha_a F$) for a single electron transfer oxidation reaction
(iii) The peak potential separation at half height ($\Delta E_{1/2}$ in mV) is 62.5/α_a.

Compton et al. derived an expression for such a process allowing both the transfer coefficient α_a and the value of k^0 to be determined [58]. Considering the single electron transfer involving the oxidation of an adsorbed species in an irreversible manner, it is possible to derive the following expressions;

$$k^0 = \left(\frac{\alpha_a F v}{RT}\right) \Big/ \left(\exp\left[\left(\frac{\alpha_a F v}{RT}\right)(E_p - E_f^0)\right]\right) \quad (5)$$

$$E_p = E_f^0 + \left(\frac{RT}{\alpha_a F}\right) ln\left(\frac{\alpha_a F v}{RT k^0}\right) \quad (6)$$

Thus for a surface-bound adsorbed species undergoing an irreversible oxidation reaction, as v (or ln v) increases, then so too does the peak potential E_p according to the relationship described by Eq. (6). This equation predicts that a plot of E_p *versus* ln v will yield a straight line of gradient $\left(\frac{RT}{\alpha_a F}\right)$ enabling α_a to be determined from the slope. If however E_p is plotted against v, then the intercept indicates the formal potential E_f^0 [59,60]. Using this value in Eq. (5) above, in conjunction with the value of α_a determined from Eq. (6), (or from (iii) above), then the rate constant k^0 can be estimated from Eq. (5). It should be noted that this approach is an alternative to the conventional one suggested by Laviron which utilises differences between anodic and cathodic peak potentials as a function of sweep rate [56,57,61]. In this work however a cathodic peak associated with peak Ia is not readily discernible.

From the results presented in Fig. 6, it is possible to estimate α_a from Eq. (6), E_f^0 from the linear extrapolation of E_p *versus* v to 0 V/s and then finally k^0. Initially, the slope of the plot of E_p *versus* ln v (See supplementary information, , Fig SI-4) was evaluated giving an α_a of 0.46 (estimated for sweep rates of > 0.05 V/s). Sweep rates above 0.05 V/s were used for this purpose, as this was the most linear section of the E_p *versus* ln v plot. Fotouhi et al. used a similar approach in their investigation of a modified MWCNT carbon paste electrode involving a surface-confined species for the detection of NADH [62]. Sweep rates above 100 mV/s were used by them to ascertain a k^0 of 2.239 s^{-1}. In the next step, extrapolation of a plot of E_p *versus* v, to 0.0 V/s yielded an intercept (E_f^0) of 0.577 V (vs SCE). Then, using these values the heterogeneous rate constant k^0 was estimated to be 4.1 s^{-1} based on an E_p of 0.6 V (vs SCE) at a sweep rate of 1 V/s from Eq. (5).

There are many mechanisms proposed for the oxidation reaction of DCF in the literature. It is often described that the mechanism of this reaction is a reversible process of $2e^-$, $2H^+$ as reported by Goyal et al., whereby 5-OH diclofenac is formed [55]. In these studies, the DCF oxidation process begins with the protonated molecule. However, at pH 7 the predominant DCF species would be the deprotonated molecule (see supplementary information , Fig SI-5). An alternative description is that given by Cid-Ceron et al. [47] and Aguilar-Lira et al. [48] involving an EC process at pH 7. Initially, the DCF reacts with water and after undergoing an oxidation reaction losing one electron and one proton. The nitrogen resonates between the creation of a double bond and formation of a radical (See supplementary information, , Scheme SI 1). This may then react with the medium (water), thus producing the irreversible DCF rupture into two products, 2,6-dichloroaniline and 2-hydroxyphenyl acetate.

3.2.2. Analytical performance

The SWV method was utilised for the determination of different concentrations of DCF solutions, using the modified SPCE-CeO_2 under the optimised experimental conditions. Following preliminary work conducted in BRB over a range of pH values, a pH of 7 was selected as optimal giving the best current response. The current values are obtained by automatically subtracting the background current. Fig. 7 shows that the peak current increases with successive additions of DCF.

The determination of the limit of detection (LOD) and limit of quantification (LOQ) of the proposed modified electrode was also performed. The calibration curve is linear in the low concentration range of 0.4–1.6 μM with the regression equation: I_p = 0.05787 C + 0.01323.

This has a correlation coefficient (R^2) of 0.9964 In the higher concentration range of 3.6–25.6 μM another very good linear relationship was obtained with the regression equation:

I_p = 0.05226 C + 0.15738, and a correlation coefficient (R^2) of 0.9969. The occurrence of two separate linear ranges for the detection of DCF was also reported by Shalauddin et al. [14]. Using differential pulse voltammetry (DPV) in conjunction with nanocellulose/f-MWCNT on glassy carbon electrodes, they studied DCF levels in pharmaceutical products and biological fluids reporting two linear calibration ranges, low (0.05–1 μM) and high (2–250 μM). These are similar ranges to those found in this work. Guzmán et al. also reported the existence of two linear ranges (low ~0–5 μM and high, 5–100 μM) in their investigation of DCF undertaken using DPV in pH 7 phosphate buffer solution [13].

No reasons were suggested however for the occurrence of the two distinct linear regimes. One possibility is that at low concentrations the adsorption of the reactant DCF species is only sufficient for a submonolayer level of reactant to adsorb, whereas at higher concentrations the reactivity is hindered as layers build up on the top or outermost surfaces, thereby shielding some reactive sites and effectively hindering electron transfer processes.

In the present investigation the LOD and LOQ were based on 3 s/m and 10 s/m respectively, where s is the standard deviation of the peak currents (n = 3, three runs) and m is the slope of the calibration curve [64]. The LOD was estimated to be 0.4 μM and 0.12 μM was found to be the LOQ. The sensitivity was determined as 0.058 μA/μM. This indicated that DCF can be estimated with a high level of confidence in the given concentration range (0.4–25.6 μM) using this SWV/SPCE-CeO_2 NP system.

3.2.3. Signal processing effects

The analytical conditions of a range of different modified electrodes for the determination of DCF using a variety of materials as the WE and a variety of nanoparticles for enhanced sensitivity are compared in Table 2. As can be observed in this Table, the LOD value that was obtained for the sensor fabricated in this work is either lower than or similar to those reported for other electrochemical sensors. However, this comparison strictly should only be carried out taking into account other factors such as sensor sensitivity, simplicity and its low cost of fabrication. Also, the difference in background correction procedure used and the number of data points utilised varies widely, as reported in Table 2. It is well known that the background correction can have a huge effect on the current response and peaks detected. However, it is rarely dealt with in the literature and consequently, comparison of LOD should not be directly undertaken without taking this into account.

Furthermore, the number of data points (not the range of concentration) selected to obtain the regression equation (and hence determine the LOD) is not the same within existing reports. However, in the majority of studies of electrochemical sensors typically the number of data points varies from 3 to 10 [1–5,15–16]. In the table above the number of data points selected for all studies was 6 or 7, and in this work, it was 7 as can be seen in Fig. 8.

It can be seen in Fig. 9, that it is necessary to carry out background correction in order to reveal the true magnitude of the peaks. It should be pointed out that in the reports cited in Table 2, no mention is made of how the background correction was carried out or it is often mentioned that it was carried out simply by subtracting the background current. Error in peak height determination is more evident at low peak sensitivities, thus generating larger inaccuracies at lower concentrations.

3.2.4. Stability and reproducibility of the modified electrode

The long term stability of the CeO_2-SPCE was evaluated by measuring the voltammetric current response of a fixed concentration of DCF (100 μM) after the modified electrode was stored for 2 weeks in a refrigerator at 4 °C and the peak current was measured every week. A relative standard deviation (R.S.D) of about 15% was observed. The reproducibility of the modified sensor was evaluated by using five independent electrodes and checking the current response of a 100 μM DCF solution. Here the R.S.D value obtained was 2.7%, indicating excellent reproducibility of the method. The repeatability of the modified electrode was investigated. The precision of the method was evaluated by repeating five sequential measurements in the same solution containing 100 μM of DCF using the same SPCE-CeO_2/NP. The R.S.D was found to be 8.5%, indicating that SPCE-CeO_2/NP is more suitable as a disposable electrode.

3.2.5. Selectivity and interfering species.

The work reported in this paper focussed on the detection of DCF in aqueous conditions using a modified SPCE-CeO_2/NP sensor together with SWV in a BRB of pH 7. In order to assess the selectivity of the method, comparison can be made to the voltammetry of DCF reported in the literature. For example, Shalauddin et al. [14] reported that diclofenac had an E_p of about 0.65 V (vs Ag/AgCl (3 M)), very close to the values found in this work, whereas dopamine displayed an E_p of about 0.42 V (vs Ag/AgCl (3 M)). Thus the peaks were separated by over 0.2 V. Ascorbic acid, displaying a well-separated peak at approximately 0.17 V(vs Ag/AgCl (3 M)) was also reported. This peak is more than 0.45 V distant from the diclofenac peak. Besides, they also reported that uric acid and various carbohydrates (fructose, glucose, lactose and sucrose), even when in 100 fold excess did not interfere with the diclofenac oxidation peak.

In the case of xanthine in biological fluids, most investigations appear to have been conducted at slightly lower pH 5 PBS solution with E_p values of near 0.8 V (vs Ag/AgCl) which is more than 0.15 V more positive than the diclofenac E_p value found in this work [20,21]. Another study using Co-doped CeO_2 nanoparticles, in an electrochemical sensor for the simultaneous determination of hypoxanthine, xanthine, and uric acid reported similar E_p values to those given in these references [23]. Guzmán et al [13] found that Ibuprofen did not interfere with DCF detection at any level. Ascorbic acid, citric acid, oxalic acid and sodium dodecyl sulfate only interfered at concentrations greater than or equal to that of DCF. Paracetamol (acetaminophen, ACOP) however was found to cause the most interference and the authors recommended the use of the standard addition method to minimize potential interference from paracetamol when determining DCF in an electrochemical sensor. For the SPCE-CeO_2/NP electrodes however it was found that it was possible to detect paracetamol, aspirin and

Table 2
Comparison of the analytical conditions of different modified electrodes for the determination of Diclofenac.

Method	Technique	Linear range ($\mu molL^{-1}$)	LOD ($\mu molL^{-1}$)	Sensitivity (μA/μM)	Reference
Reduced graphene oxide (rGO)/$Co(OH)_2$nano-flakes rGO/CHNF/CPE	C.V	3.7–140	0.05	1.370	[6]
Au-PtNPs/f-MWCNTs/AuE	DPV	0.5–1000	0.30	0.012	[11]
MWCNTSs/$Cu(OH)_2$ NPs/IL /GCE	DPV	0.18–119	0.04	0.014	[12]
MWCNT/CPE	DPV	0.1–100	0.001	0.299	[13]
f-MWCNTs/nanocellulose/GCE	DPV	0.05–250	0.012	2.619	[14]
CeO_2-SPCE	SWV	0.1–25.6	0.40	0.058	This work

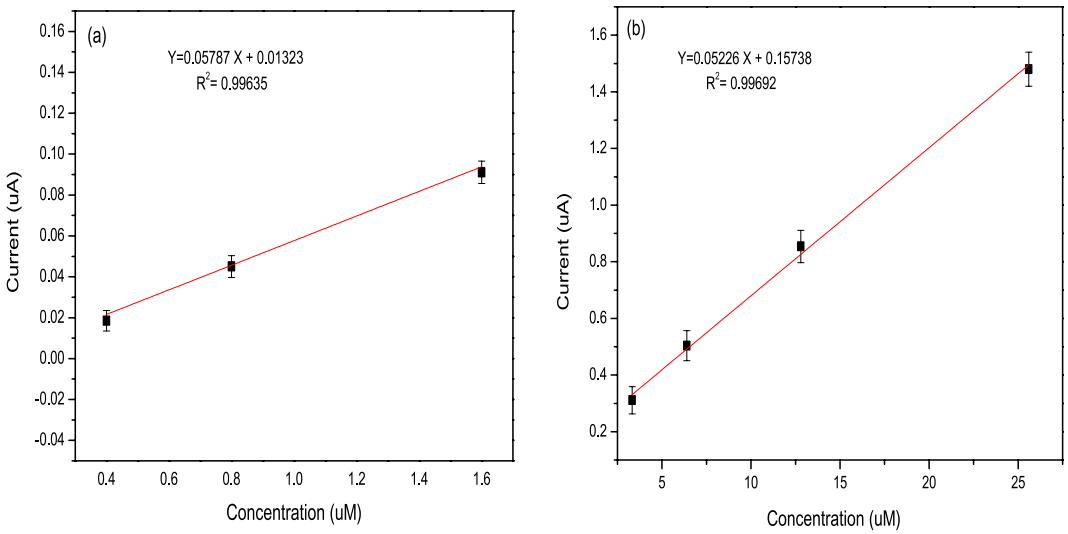

Fig. 8. Plots showing linear dependence of the anodic peak current as a function of DCF concentration in the range of (a) 0.4–1.6 μM and (b) 3.3–25.6 μM (number of replicates = 3).

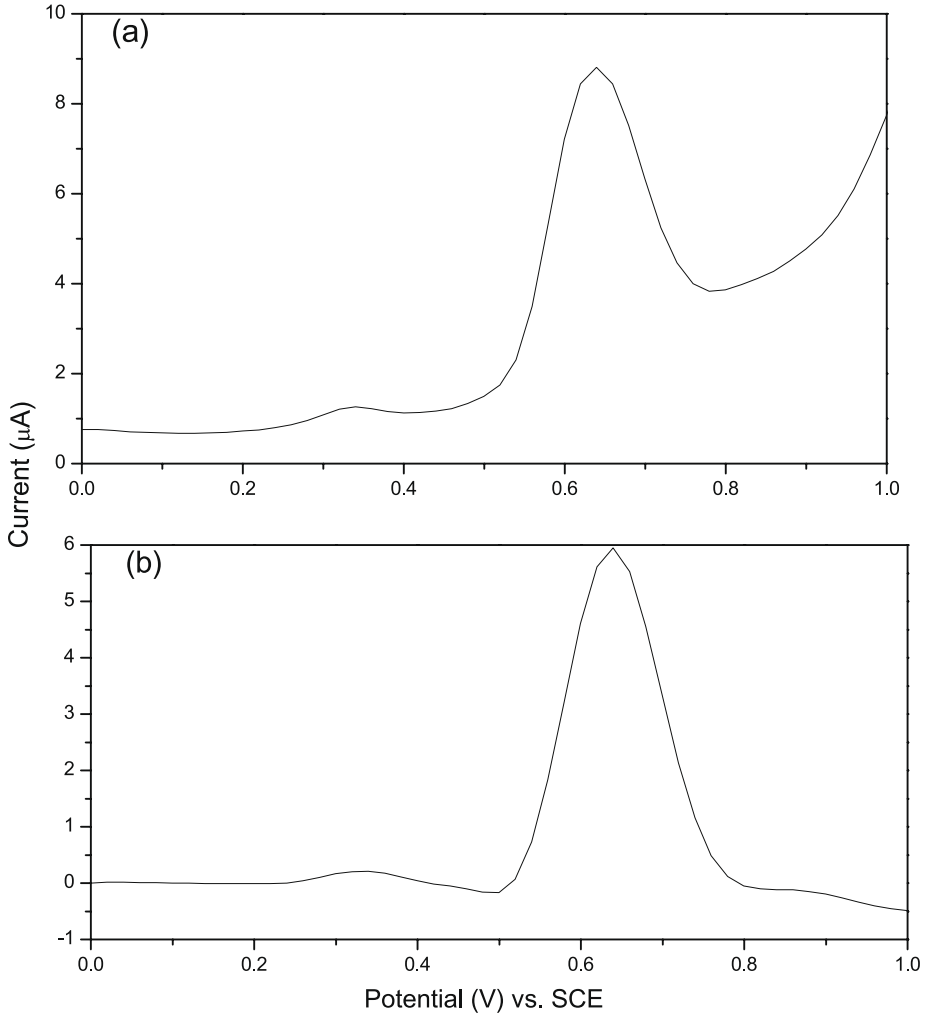

Fig. 9. Square wave voltammograms of DCF 10 mg/L (a) without background correction and (b) with background correction. Using the SPCE-CeO_2 as the WE, carbon ink CE and an external SCE as a RE. SWV analysis conditions: f = 40 Hz, E_{step} = 20 mV and E_{pulse} = 25 mV. SWV performed in BRB (pH = 7).

caffeine in a common pharmaceutical product using SWV under the same conditions [63]. None of these compounds showed a current response near the DCF value of 0.6 V (Vs SCE) (as is evident in the supplementary information, Fig SI-6). Further exploration of the selectivity of the modified SPCE-CeO_2/NP sensor and its response to a range of other compounds that may be found in natural or wastewaters would be worthwhile.

4. Conclusions

The SPCE-CeO_2/SWV electrochemical method outlined in this paper shows many advantages over other sensors reported in the literature; notably a simple fabrication process, and hence the possibility of large scale-production, use of relatively low-cost materials, and the potential for use over wide concentration ranges of DCF. The main advantage of this electrochemical sensor is that it can be used portably, possibly in the field with a small portable potentiostat instrument utilising a nanoparticle sized catalyst (CeO_2) that is relatively inexpensive and abundant, in conjunction with a commercially available SPCE. From a practical perspective the main advantage of SWV over many other analytical techniques is that accurate analyses can be carried out in a short time (of the order of seconds as fast scan rates can be used) without the need for bulky expensive equipment, solvents and special gases. When the baseline correction (the moving average) in a high potential region is performed, there is an inherent interference with the peak height of the analyte, resulting from the presence of high background currents due to the onset of oxygen evolution and possibly carbon oxidation reactions, thereby making the determination of compounds above +0.8 V unreliable. In the case of DCF however which undergoes an oxidation reaction at around 0.2 V less than this figure, this problem is greatly diminished using SWV combined with background correction. This allows an accurate assessment of DCF levels to be undertaken with good sensitivity and reproducibility. This approach shows considerable promise as a means of carrying out a quick and accurate assessment of DCF levels in environmental water samples, although it may also possibly be extended to the determination of DCF levels in pharmaceutical and/or samples of biological interest. Finally, an investigation of the selectivity of the modified SPCE-CeO_2 NP sensor is worth pursuing to accurately determine the role of possible interfering species and EIS analysis as another method to determine k^0 values for charge transfer reactions.

CRediT authorship contribution statement

Rafaela C. de Carvalho: Writing - original draft, Conceptualization, Methodology, Software, Investigation, Validation, Visualization, Data analysis. **Anthony J. Betts:** Writing - review & editing, Supervision, Conceptualization, Data analysis. **John F. Cassidy:** Writing - review & editing, Supervision, Conceptualization, Data analysis.

Declaration of Competing Interest

The authors declare that they have no known competing financial interests or personal relationships that could have appeared to influence the work reported in this paper.

Acknowledgements

The authors gratefully acknowledge the Fiosraigh Dean of Graduate Studies award from Technological University Dublin to R de Carvalho, the ESHI, FOCAS Institute and COST Action MP1407 (e-MINDS) support.

Appendix A. Supplementary data

Supplementary data to this article can be found online at https://doi.org/10.1016/j.microc.2020.105258.

References

[1] M.R. Siddiqui, Z.A. Al Othman, N. Rahman, Analytical techniques in pharmaceutical analysis: a review, Arabian, J Chem. 10 (2017) S1409–S1421.
[2] P.N. Badyal, C. Sharma, N. Kaur, R. Shankar, A. Pandey, R.K. Rawal, Analytical techniques in simultaneous estimation: an overview, Austin J. Anal. Pharm. Chem. 2 (2015) 1037–1040.
[3] B.J. Sanghavi, A.K. Srivastava, Simultaneous voltammetric determination of acetaminophen, aspirin and caffeine using an in situ surfactant-modified multiwalled carbon nanotube paste electrode, Electrochim. Acta 55 (2010) 8638–8648.
[4] J.M. Freitas, D.L.O. Ramosa, R.M.F. Sousa, T.R.L.C. Paixão, M.H.P. Santana, R.A.A. Munoz, E.M. Richter, A portable electrochemical method for cocaine quantification and rapid screening of common adulterants in seized samples, Sens. Actuators, B 243 (2017) 557–565.
[5] Q.C. Chu, L.M. Jiang, X.H. An, J.N. Ye, Rapid determination of acetaminophen and p-aminophenol in pharmaceutical formulations using miniaturized capillary electrophoresis with amperometric detection, Anal. Chim. Acta 606 (2008) 246–251.
[6] M. Mohamed, A. El-Wekil, A. Saad, H.H. Alkahtani, R.H. Ali, A.M. Mahmoud, Advanced sensing nanomaterials based carbon paste electrode for simultaneous electrochemical measurement of esomeprazole and diclofenac sodium in human serum and urine samples, J. Mol. Liq. 262 (2018) 495–503.
[7] S. Fletcher, Screen-Printed Carbon Electrodes, in Electrochemistry of Carbon Electrodes, Wiley-VCH Verlag GmbH & Co. KGaA, Weinheim, Germany, 2015, pp. 425–444.
[8] R.T. Kachoosangi, G.G. Wildgoose, R.G. Compton, Adsorptive stripping voltammetric determination of 4-hexylresorcinol in pharmaceutical products using multiwalled carbon nanotube based electrodes, Electroanalysis 20 (2008) 1714–1719.
[9] S. Carrara, V.V. Shumyantseva, A.I. Archakov, B. Samori, Screen-printed electrodes based on carbon nanotubes and cytochrome P450scc for highly sensitive cholesterol biosensors, Biosens. Bioelectron. 24 (2008) 148–152.
[10] R.T. Kachoosangi, G.G. Wildgoose, R.G. Compton, Sensitive adsorptive stripping voltammetric determination of paracetamol at multiwalled carbon nanotube modified basal plane pyrolytic graphite electrode, Anal. Chim. Acta 618 (2008) 54–60.
[11] M.M. Eteya, G.H. Rounaghi, B. Deiminiat, Fabrication of a new electrochemical sensor based on AuPt bimetallic nanoparticles decorated multi-walled carbon nanotubes for determination of diclofenac, Microchem J 144 (2019) 254–260.
[12] M. Arvand, T.M. Gholizadeh, M.A. Zanjanchi, MWCNTs/$Cu(OH)_2$ nanoparticles/IL nanocomposite modified glassy carbon electrode as a voltammetric sensor for determination of the non-steroidal anti-inflammatory drug diclofenac, Mat. Sci. Eng. C 32 (2012) 1682–1689.
[13] M.F. Guzmán, L.H.M. Huizar, C.A.G. Vidal, G.R. Morales, G.A. Á. Romero, A Box-Behnken optimized methodology for the quantification of diclofenac using a carbon paste-multiwalled carbon nanotubes electrode, Current Anal. Chem. 15 (2019) 294–304.
[14] M. Shalauddin, A. Shamima, W.J. Basirun, S. Bagheri, N.S. Anuar, M.R. Johan, Hybrid nanocellulose/f-MWCNTs nanocomposite for the electrochemical sensing of diclofenac sodium in pharmaceutical drugs and biological fluids, Electrochim. Acta 304 (2019) 323–333.
[15] Erin Jo Tiedeken, Alexandre Tahar, Brendan McHugh, Neil J. Rowan, Monitoring, sources, receptors, and control measures for three European Union watch list substances of emerging concern in receiving waters – a 20 year systematic review, Sci. Total Environ. 574 (2017) 1140–1163.
[16] C. Batchelor-McAuley, G.G. Wildgoose, The influence of substrate effects when investigating new nanoparticle modified electrodes exemplified by the electroanalytical determination of aspirin on NiO nanoparticles supported on graphite, Electrochem. Commun. 10 (2008) 1129–1131.
[17] M. Aklilu, M. Tessema, M. Redi-Abshiro, Indirect voltammetric determination of caffeine content in coffee using 1,4-benzoquinone modified carbon paste electrode, Talanta 76 (2008) 742–746.
[18] M. Khairy, B.G. Mahmoud, C.E. Banks, Simultaneous determination of codeine and its co-formulated drugs acetaminophen and caffeine by utilising cerium oxide nanoparticles modified screen-printed electrodes, Sens. Actuators B 259 (2018) 142–154.
[19] H. Ibrahim, M. Ibrahim, Y. Temerk, A novel megestrol acetate electrochemical sensor based on conducting functionalized acetylene black–CeO_2 NPs nanohybrids decorated glassy carbon, Talanta 200 (2019) 324–332.
[20] H. Ibrahim, Y. Temerk, Sensitive electrochemical sensor for simultaneous determination of uric acid and xanthine in human biological fluids based on the nanoboron doped ceria modified, J. Electroanal. Chem. 780 (2016) 176–186.
[21] H. Ibrahim, Y. Temerk, A novel electrochemical sensor based on B doped CeO_2 nanocubes modified glassy carbon microspheres paste electrode for individual and simultaneous, Sens. Actuators, B 232 (2016) 125–137.
[22] Y. Temerk, H. Ibrahim, A new sensor based on In doped CeO_2 nanoparticles modified glassy carbon paste electrode for sensitive determination of uric acid in biological fluids, Sens. Actuators, B 224 (2016) 868–877.
[23] N. Lavanya, C. Sekar, R. Murugan, G. Ravi, An Ultrasensitive Electrochemical Sensor for Simultaneous Determination of Xanthine, Hypoxanthine and Uric Acid Based on Co Doped CeO2 Nanoparticles, Mater. Sci. Eng. C Mater. Biol. Appl. 1 (65) (2016) 278–286.

[24] C.M.A. Brett, A.M.O. Brett, Electroanalysis, first ed., Oxford, 1998.
[25] A.J. Bard, L.R. Faulkner, Electrochemical Methods: Fundamentals and Applications, second ed, Wiley, 2000.
[26] K. Crowley, J. Cassidy, Trace analysis of lead at a nafion-modified electrode using square-wave anodic stripping voltammetry, Electroanalysis 14 (2002) 1077–1082.
[27] R.O. Kadara, N. Jenkinson, C.E. Banks, Characterisation of commercially available electrochemical sensing platforms, Sens. Actuators, B 138 (2009) 556–562.
[28] N. Thiyagarajan, J.-L. Chang, K. Senthilkumar, J.-M. Zen, Disposable electrochemical sensors: a mini review, Electrochem. Commun. 38 (2014) 86–90.
[29] M. Moreno, A.S. Arribas, E. Bermejo, M. Chicharro, A. Zapardiel, M.C. Rodríguez, Y. Jalit, G.A. Rivas, Selective detection of dopamine in the presence of ascorbic acid using carbon nanotube modified screen-printed electrodes, Talanta 80 (2010) 2149–2156.
[30] M. Jakubowska, Signal processing in electrochemistry, Electroanalysis 23 (2011) 553–572.
[31] N.P.C. Stevens, M.B. Rooney, A.M. Bond, S.W. Feldberg, A comparison of simulated and experimental voltammograms obtained for the [Fe(CN)6]3-/4-couple in the absence of added supporting electrolyte at a rotating disk electrode, J. Phys. Chem. 105 (2001) 9085–9093.
[32] A. Garcia-Miranda Ferrari, C.W. Foster, P.J. Kelly, D.A.C. Brownson, C.E. Banks, Determination of the electrochemical area of screen-printed electrochemical sensing platforms, Biosensors 8 (2018) 53–58.
[33] A. Al Kumar, B.E.K. Swamy, T.S. Rani, P.S. Ganesh, Y.P. Raj, Voltammetric determination of catechol and hydroquinone at poly(murexide) modified glassy carbon electrode, Mater. Sci. Eng., C 98 (2019) 746–752.
[34] M.R. El-Zahry, M.F.B. Ali, Enhancement effect of reduced graphene oxide and silver nanocomposite supported on poly brilliant blue platform for ultra-trace voltammetric analysis of rosuvastatin in tablets and human plasma, RSC Adv. 9 (2019) 7136–7146.
[35] M.F.B. Ali, M.R. El-Zahry, A comparative study of different electrodepositedNiCo2O_4 microspheres anchored on a reduced graphene oxide platform: electrochemical sensor for anti-depressant drug venlafaxine, RSC Adv. 9 (2019) 31609–31620.
[36] C.E. Banks, T.J. Davies, G.G. Wildgoose, R.G. Compton, Electrocatalysis at graphite and carbon nanotube modified electrodes: edge-plane sites and tube ends are the reactive sites, Chem. Commun. 7 (2005) 829–836.
[37] R.S. Nicholson, Anal. Chem. 37 (1965) 1351–1355.
[38] A. Morrin, A.J. Killard, M.R. Smyth, Electrochemical characterization of commercial and home-made screen-printed carbon electrodes, Anal. Lett. 36 (2003) 2021–2039.
[39] T.A. Swaddle, Homogeneous versus heterogeneous self-exchange electron transfer reactions of metal complexes: insights from pressure effects, Chem. Rev. 105 (2005) 2573–2608.
[40] A. Grimaldi, G. Heijo, E. Mendez, A multiple evaluation approach of commercially available screen-printed nanostructured carbon electrodes, Electroanalysis 26 (2014) 1684–1693.
[41] P. Fanjul-Bolado, D. Hernández-Santos, P.J. Lamas-Ardisana, A. Martín-Pernía, A. Costa-García, Electrochemical characterization of screen-printed and conventional carbon paste electrodes, Electrochim. Acta 53 (2008) 3635–3642.
[42] J. Trijueque, J.J. García-Jareño, J. Navarro-Laboulais, A. Sanmatías, F. Vicente, Ohmic drop of Prussian-blue/graphite + epoxy electrodes, Electrochim. Acta 45 (4-5) (1999) 789–795.
[43] A.A. Karyakin, Prussian blue and its analogues: electrochemistry and analytical applications, Electroanalysis 13 (2001) 813–819.
[44] Y. Yi, G. Weinberg, M. Prenzel, M. Greeiner, S. Heumann, S. Becker, R. Schlogl, Electrochemical corrosion of a glassy carbon electrode, CatalysisToday 295 (2017) 32–40.
[45] X. Liu, Z. Sun, S. Cui, P. Du, Cuprous oxide thin film directly electrodeposited from a simple copper salt on conductive electrode for efficient oxygen evolution reaction, Electrochim. Acta 187 (2016) 381–388.
[46] A. Rojas-Hernández, M.T. Ramírez, I. González, J.G. Ibáñez, Multi-dimensional predominance-zone diagrams for polynuclear chemical species, Anal. Chim. Acta 259 (1992) 95–104.
[47] M.M. Cid-Cerón, D.S. Guzmán-Hernández, M.T. Ramírez-Silva, A. Galano, M. Romero-Romo, M. Palomar-Pardavé, New insigths on the kinetics and mechanism of the electrochemical oxidation of diclofenac in neutral aqueous medium, Electrochim. Acta 199 (2016) 92–98.
[48] G.Y. Aguilar-Lira, G.A. Álvarez-Romero, A. Zamora-Suárez, M. Palomar-Pardavé, A. Rojas-Hernández, J.A. Rodríguez-Ávila, M.E. Páez-Hernández, New insights on diclofenac electrochemistry using graphite as working electrode, J. Electroanal. Chem. 794 (2017) 182–188.
[49] S.M. Sayyah, M.M. El-Rabiey, H. El-Feky, A.F. Gaber, Electrochemical polymerization of 2,6-dichloroaniline and characterization of the obtained polymer, Int. J. Polym. Mater. Polym. Biomater. 55 (2006) 457–476.
[50] E. Brillas, S. Garcia-Segura, M. Skoumal, C. Arias, Electrochemical incineration of diclofenac in neutral aqueous medium by anodic oxidation using Pt and boron-doped diamond anodes, Chemosphere 79 (2010) 605–612.
[51] R.C. de Carvalho, A.J. Betts, J.F. Cassidy, Formation of p–n junctions in nanoparticle cerium oxide electrolytic cells displaying memristive switching behaviour, Phys. Chem. Chem. Phys 22 (2020) 4216–4224.
[52] B. Choudhury, P. Chetri, A. Choudhury, Oxygen defects and formation of Ce3 + affecting the photocatalytic performance of CeO2 nanoparticles, RSC Adv. 4 (2014) 4663–4671.
[53] S.X. Guo, S.F. Zhao, A.M. Bond, J. Zhang, Simplifying the evaluation of graphene modified electrode performance using rotating disk electrode voltammetry, Langmuir 28 (2012) 5275–5285.
[54] E. Costa-Rama, H.P.A. Nouws, C. Delerue-Matos, M.C. Blanco-Lopez, M.T. Fernandez-Abedul, Preconcentration and sensitive determination of the anti-inflammatory drug diclofenac on a paper-based electroanalytical platform, Anal. Chim. Acta 1074 (2019) 89–97.
[55] R.N. Goyal, S. Chatterjee, B. Agrawal, Electrochemical investigations of diclofenac at edge plane pyrolytic graphite electrode and its determination in human urine, Sens. Actuators, B 145 (2010) 743–748.
[56] E. Laviron, General expression of the linear potential sweep voltammogram in the case of diffusionless electrochemical systems, J. Electroanal. Chem. Interfacial Electrochem. 101 (1979) 19–28.
[57] M.J. Honeychurch, G.A. Rechnitz, Voltammetry of adsorbed molecules. Part 2: irreversible redox systems, Electroanalysis 10 (1998) 453–457.
[58] R.G. Compton, C. Batchelor-McAuley, E.J.F. Dickinson, Understanding Voltammetry: Problems and solutions, first ed. (2012) pp. 71-75.
[59] L. Fotouhi, M. Fatollahzadeh, M.M. Heravi, Electrochemical behavior and voltammetric determination of sulfaguanidine at a glassy carbon electrode modified with a multi-walled carbon nanotube, Int. J. Electrochem. Sci.. 7 (2012) 3919–3928.
[60] L. Fotouhi, M. Nemati, M.M. Heravi, Electrochemistry and voltammetric determination of furazolidone with a multi-walled nanotube composite film-glassy carbon electrode, J. Appl. Electrochem. 41 (2011) 137–142.
[61] E. Wudarska, E. Chrzescijanska, E. Kusmierek, J. Rynkowski, Electrochemical behavior of 2-(p-isobutylphenyl)propionic acid at platinum electrode, Int. J. Electrochem. Sci. 10 (2015) 9433–9442.
[62] L. Fotouh, F. Raei, M.M. Heravi, D. Nematollahi, Electrocatalytic activity of 6,7-dihydroxy-3-methyl-9-thia-4,4a-diazafluoren-2-one/multi-wall carbon nanotubes immobilized on carbon paste electrode for NADH oxidation: application to the trace determination of NADH, J. Electroanal. Chem. 639 (2010) 15–20.
[63] R.C. de Carvalho, Synthesis and Novel Applications of Cerium Dioxide, PhD Thesis Technological University Dublin, 2019.
[64] B. Yilmaz, S. Kaban, B.K. Akcay, U. Ciltas, Differential pulse voltammetric determination of diclofenac in pharmaceutical preparations and human serum, Braz. J. Pharm. Sci. 51 (2015) 285–294.